

FLUID DYNAMIC EFFICIENCY OF A HIGH PERFORMANCE MULTI-VALVE INTERNAL COMBUSTION ENGINE DURING THE INTAKE PHASE

Influence of Valve-Valve Interference Phenomena

by

Angelo ALGIERI

Mechanics Department, University of Calabria, Arcavacata di Rende (CS), Italy

Original scientific paper
DOI: 10.2298/TSC1120730221A

The purpose of the present work is the analysis of the fluid dynamic behaviour of a high performance internal combustion engine during the intake phase. In particular, a four-valve spark-ignition engine has been characterised at the steady flow rig. Dimensionless discharge coefficients have been used to define the global fluid dynamic efficiency of the intake system, while the laser-Doppler anemometry technique has been employed to evaluate the mean flow in the valve curtain area and to characterise the interference phenomena between the two intake valves.

The investigation has shown the significant influence of the valve lift on the volumetric efficiency of the intake apparatus. Moreover, the experimental analysis has highlighted that the valve-valve interference phenomena have a relevant impact on the head breathability, on the flow development within the combustion chamber and on the velocity standard deviations.

Key words: *internal combustion engines, intake phase, flow coefficients, laser-Doppler anemometry, valve deactivation, interference phenomena*

Introduction

Nowadays, the detailed characterisation of the fluid dynamic behaviour of internal combustion engines represents an essential step to developing and optimising modern internal combustion engines (ICE) [1-5]. A profound knowledge of the intake process, in fact, is necessary both when the purpose is to meet the more and more stringent regulations on the exhaust gas emissions and when the goal is to increase the performances of race engines [1, 6-8]. Specifically, in multi-valve high performance engines, extreme head designs are often adopted in order to maximise torque and power. The distance between the inlet valves is significantly decreased and noticeable valve-to-valve interference phenomena are produced during the intake phase.

Furthermore, to reduce fuel consumption and increase engine efficiency at low loads, the deactivation of an inlet valve is considered an interesting strategy [9-12]. As an example, Moore *et al.* [9] investigated the influence of valve deactivation strategy on the fuel consumption and emissions considering a 2 litre gasoline direct injection (GDI) engine with a dual independent cam phasing (DICP). The analysis showed that the use of valve deactivation guarantees a significant improvement in fuel economy with respect to the base engine for loads lower than 6

bar and an interesting improvement in combustion stability. Specifically, the authors reported up to 11% reduction in brake specific fuel consumption at 2000 rpm for the engine fuelled with 91 RON gasoline. Similar results were found by Patel *et al.*, that focused their attention on a single-cylinder direct injection spark ignition engine fuelled with 95 RON gasoline [12]. The experimental analysis demonstrated that, at low load (2.7 bar) and speed (2000 rpm), the deactivation of one of the two valves and the adoption of reduced valve lift assures a 5.8% decrease in the indicated specific fuel consumption compared with the standard engine operation.

The results confirm that engine performances are noticeably effected by the in-cylinder flow and that the characterisation of the intake phase is fundamental. To this purpose, several investigative tools, based on computational fluid dynamics (CFD) codes or experimental approaches [13-17], are available to examine in detail the fluid dynamic behaviour of real engines. Specifically, the steady flow rig is a widely employed tool, due to the proper simulation of the real phases and the possibility of using real engines and components [18-22].

Studies are typically based on global and/or local analyses. To this purpose, dimensionless flow coefficients [23-26] are adopted to provide global information on the fluid dynamic efficiency of engines during the intake process and supply useful advice to engine designers and tuners on the location and sizing of ducts and valves [21]. At the same time, non-intrusive laser-Doppler anemometry (LDA) and particle image velocimetry (PIV) techniques [27-30] can be used to define in more detail the flow distribution within the ducts and cylinders of modern internal combustion engines.

The present work aims at analysing the fluid dynamic behaviour of a high performance four-valve spark-ignition engine during the intake phase and evaluating the interference phenomena between the intake valves and the influence of the valve deactivation on the head breathability. In fact, few quantitative studies on the effect of the valve-to-valve interaction and on the influence of the valve deactivation on the engine permeability are available in the literature, despite the significant impact on the engine performances. To this purpose, the intake system was characterised at a steady flow rig adopting the dimensionless discharge coefficients and the LDA technique.

Experimental apparatus

Table 1. Main engine characteristics

Engine	Four-stroke spark-ignition
Number of cylinders, N_c	10
Number of valves per cylinder, N_v	4
Stroke/bore, L/B	0.431
Intake valve diameter/bore, D_i/B	0.417
Exhaust valve diameter/bore, D_e/B	0.349

The experimental analysis has been focused on a high performance ICE. The engine is part of a multi-cylinder race engine, characterized by four valves per cylinder. Table 1 lists the main engine characteristics.

The fluid dynamic efficiency of the intake apparatus has been investigated at a steady flow rig, enabling air to be forced through the system by means of a blower while the valve lift is fixed to a selected value (fig. 1). Temperature and pressure transducers have been used to characterise

the conditions of the ambient and inside the cylinder, while a laminar flow meter system has been adopted to measure the global mass flow rate [31].

The facility also enables local velocity measurements with LDA. To this purpose, optical access to the cylinder was obtained through a window perpendicular to the cylinder axis. The

LDA system is a one-colour system (*i. e.* capable of measuring one component of the velocity) in a back-scattering configuration, with a Bragg-cell frequency shifter. The system uses a continuous argon-ion laser as light source (2 W on the green line, at $\lambda = 514.5$ nm) and optical fibres for both transmitting and collecting optics. The transmitting optics include a beam splitter and a focusing lens, while the receiving optics consists of a focusing lens, a photodetector and an interference filter. The main geometrical data of the optical system are given in tab. 2.

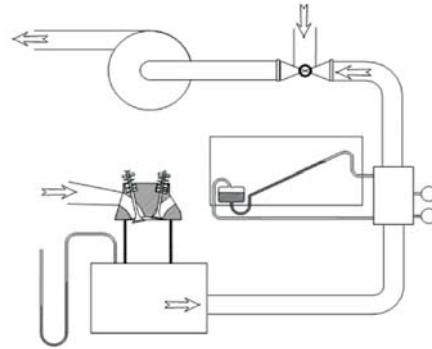


Figure 1. Steady flow rig

If a frequency shifter module is used, the number of fringes depends on other parameters, such as record length, centre frequency, and band width used by the signal processor. In the case of the reported measurements, the resulting number of fringes was 48.

The movement of the LDA probe is obtained by using a micrometer x-y traversing system. The probe can also be rotated around its axis and moved vertically (z-axis). A dedicated signal processor, which performs fast-Fourier transform (FFT) processing of the original signal in order to extract the Doppler frequency, is used for the analysis of the Doppler signal and ensures rejection of the signal produced by different particles that may be present within the measuring volume at the same time. The processor is linked to a computer in order to store and analyse the data.

Table 2. Optical system data

Beam spacing	38	mm
Focal length	400	mm
Probe volume width	0.194	mm
Probe volume length	4.09	mm
Number of fringes	35	
Fringe spacing	5.42	μm

For the seeding system a fluidised bed-like scheme was employed. A fraction of the inlet air is first dried and then passed through a horizontal porous diaphragm on the top of which a layer of silica “micro-balloons” is deposited. The air stream then carries the particles and is subsequently mixed with the main intake air at the engine inlet.

Methodology

A twofold approach has been employed to analyse the fluid dynamic behaviour of the intake system. The engine head has been examined in terms of global performances and in terms of local velocity measurements. In particular, the discharge coefficients are used to define the head breathability, while the LDA technique is adopted to determine the flow field inside the combustion chamber.

The configurations with both inlet valves open and with only one valve open have been compared in order to evaluate the interference phenomena between the two intake valves and to study the effect of the valve deactivation strategy.

Discharge coefficients

The discharge coefficients have been used to define the global fluid dynamic efficiency of the intake system [1]. Specifically, the dimensionless coefficient is defined as the ratio of the measured mass flow rate \dot{m}_{meas} to reference mass flow rate \dot{m}_r :

$$C_d = \frac{\dot{m}_{\text{meas}}}{\dot{m}_r} \quad (1)$$

If the flow is subsonic, the reference mass flow rate is given by:

$$\dot{m}_r = A_r \frac{p_0}{\sqrt{RT_0}} \left(\frac{p_C}{p_0} \right)^{\frac{1}{\gamma}} \sqrt{\frac{2\gamma}{\gamma-1} \left[1 - \left(\frac{p_C}{p_0} \right)^{\frac{\gamma-1}{\gamma}} \right]} \quad (2)$$

while, if the flow is choked, the mass flow is formalised as:

$$\dot{m}_r = A_r \frac{p_0}{\sqrt{RT_0}} \sqrt{\gamma} \left(\frac{2}{\gamma+1} \right)^{\frac{\gamma+1}{2(\gamma-1)}} \quad (3)$$

where p_0 is the intake system pressure, p_C – the cylinder pressure, T_0 – the intake system temperature, and A_r – the reference area.

Specifically, the reference area A_{ref} is the valve curtain area and, therefore, it is a linear function of valve lift L_v [18]:

$$A_r = \pi D_v L_v \quad (4)$$

Furthermore, absolute discharge coefficients C_{abs} were defined to characterise the intake system efficiency independently of the valve lift [32]:

$$C_{\text{abs}} = \frac{\phi_{\text{Am}}}{\phi_{\text{Ad}}} \quad (5)$$

where ϕ_{Ad} represents the dimensionless theoretical flow rate downstream of the valve, based on the isentropic flow condition:

$$\phi_{\text{Ad}} = \sqrt{\frac{2}{\gamma-1} \left[\left(\frac{p_C}{p_0} \right)^{\frac{2}{\gamma}} - \left(\frac{p_C}{p_0} \right)^{\frac{\gamma+1}{\gamma}} \right]} \quad (6)$$

while ϕ_{Am} is the dimensionless actual flow rate, averaged over the dimensionless valve lift:

$$\phi_{\text{Am}} = \frac{\int_0^{(L_v/D_v)_{\text{max}}} \frac{\dot{m}_{\text{meas}}}{A_r \rho_0 a_0} d \frac{L_v}{D_v}}{\left(\frac{L_v}{D_v} \right)_{\text{max}}} \quad (7)$$

where ρ_0 is the air density and a_0 – the sound speed.

Measurements have been taken for a fixed ambient-cylinder pressure drop (7.3 kPa), while the dimensionless valve lift (L_v/D_v) has been set in the 0.050-0.400 interval. The overall uncertainty of dimensionless flow coefficients – evaluated according to literature [33, 34] – was consistently lower than 3%, and it decreased with valve lift.

LDA Measurements

The local characterisation of the flow around the valve curtains has been achieved by defining 16 measuring points around each intake valve (fig. 2). The measuring points are di-

vided into four sectors, which are referred to as sector A (valve-wall interaction zone), sector B (backward flow zone), sector C (valve-valve interaction zone), and sector D (forward flow zone).

At each point, two velocity components (along the x- and y- directions) have been recorded in a plane perpendicular to the valve axis. Ten thousand samples have been collected for each velocity component. The relative uncertainty on the LDA measurements, which is mainly due to the set-up of the electronic system, was lower than 2.2% [35, 36]. The valve lift has been fixed at $L_v/D_v = 0.375$ with an ambient-cylinder pressure drop $\Delta p = 7.3$ kPa, and the measuring plane has been located at 3/4 of the valve lift. To verify the previous measurements, a third component has been acquired and it has been compared to the value calculated from the x and y components, recording a good agreement.

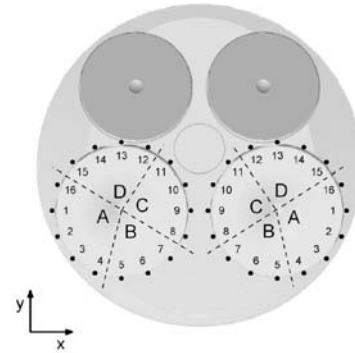


Figure 2. Measuring points around the intake valves

Results

The global fluid dynamic efficiency of the four-valve ICE has been investigated in terms of discharge coefficients as a function of the dimensionless valve lift (L_v/D_v). To this purpose, the wide open throttle (WOT) configuration has been considered and the ambient-cylinder pressure drop Δp has been set to 7.3 kPa.

Figure 3 compares the head permeability of the configurations with both inlet valves open and with only one valve open. The analysis highlights the presence of three regions, which correspond to different flow regimes, in line with the literature [1, 37]. In particular, for low valve lift, high values of the discharge coefficient and a progressive increase with the valve lift are observed. In these conditions the flow remains attached to the valve seat and head, due to the high viscous phenomena, and the entire curtain area is properly used. When the valve lift increases, a flow separation occurs at the valve head. As a consequence, a reduction in the effective flow area is produced and a progressive decrease in the head volumetric performances is registered. Successively, the presence of separation phenomena also at the valve seat reduces the fluid dynamic efficiency of the intake system with a further fall in the discharge coefficient.

Furthermore, the results put in evidence the large influence of interference phenomena between the two valves on the global efficiency of the intake system. Specifically, the absence of flow interactions between the two intake valves leads to a better filling of the cylinder when a single valve is open and $L_v/D_v \leq 0.275$. For higher lift, the previous trend is inverse, probably due to significant irregularities that are generated in the flow at the bifurcation of the intake ducts when only one valve is open. The largest differences are registered in the valve lift range 0.200-0.225, with a 6% higher value when a valve is deactivated.

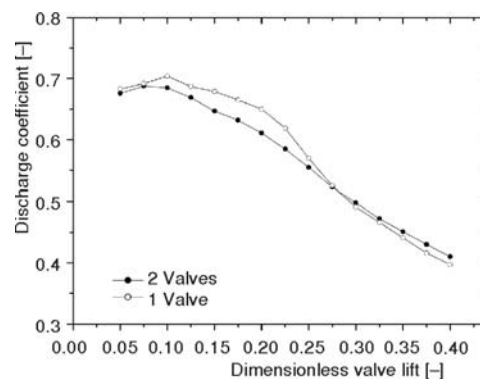


Figure 3. Influence of valve deactivation and interference phenomena on discharge coefficient. WOT configuration

Table 3 shows the absolute and maximum discharge coefficients for the two configurations. The data illustrate that higher values are registered when only one valve is open and that the difference between the two arrangements is about 1.8% and 2.7% in terms of absolute and maximum discharge coefficients, respectively. Furthermore, the analysis put in evidence that when $L_v/D_v \leq 0.225$ the discharge coefficients maintain values larger than the absolute coefficient, which corresponds to about 82.5% of the maximum discharge coefficient.

Table 3. Absolute and maximum discharge coefficients for the intake system

Analysed system	2 valves open	1 valve open
Throttle configuration	WOT	WOT
Absolute discharge coefficient, $C_{d\text{Abs}}$	0.571	0.581
Maximum discharge coefficient, $C_{d\text{max}}$	0.688	0.706

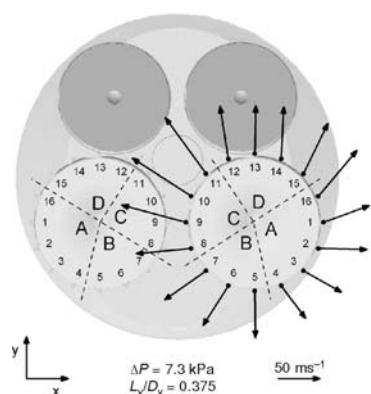


Figure 4. Velocity vectors around the intake valve when the other inlet valve is deactivated

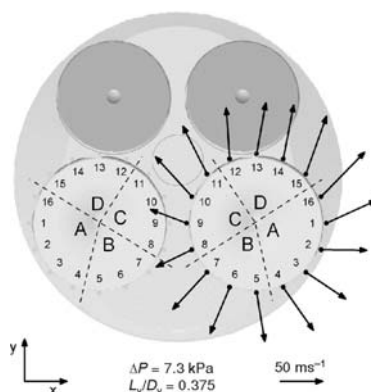


Figure 5. Velocity vectors around the intake valve when the two valves are open

To examine the flow distribution within the combustion chamber and to evaluate the influence of the valve-valve interaction in more detail, the LDA technique has been adopted. Specifically, measurements around the intake valve curtain have been carried out by fixing the valve lift ratio at $L_v/D_v = 0.375$ and by locating the measuring plane at 3/4 of the lift. The ambient-cylinder pressure drop has been imposed equal to 7.3 kPa and the WOT configuration has been considered.

Figure 4 highlights the mean velocity distribution around the intake valve when the other inlet valve is completely deactivated. The mean flow appears quite uniform, with lower velocities registered in sector A and the maximum values found towards the centre of the combustion chamber (sector C). Furthermore, the figure shows that the mean velocity direction is close to the radial direction, with some deviation at points 8-9 (owing to the intake duct orientation), on the arc 15-3 (due to the influence of the cylinder wall), and at points 12-14 (due to the wake of the valve stem).

A significant distortion in the mean flow is registered when both valves are open (fig. 5). Specifically, the valve-valve interference phenomena produce a significant decrease in the mean velocity magnitudes and a reorientation of the velocity vectors towards the y-axis in region C. The comparison in the valve-valve interaction zone put in evidence a mean 30% reduction in the velocity magnitudes when both intake valves are open and a 43% decrease at point 9, where the largest interference phenomena are present. When the two valves are open the higher velocities are registered in the region between points 10 and 1, with the maximum located at point 16 (73.5 m/s).

The influence of the valve-valve interference phenomena can be observed also on the RMS velocity distribution in the valve curtain area. To this purpose, fig. 6 shows the velocity standard deviation on the radial velocity for the two head configurations. When a valve is deactivated, more uniform standard deviations are observed. The highest RMS values are found in region B as a result of the high distortion in the flow pathlines due to the flow inversion in the intake duct, while the arc 10-15-2 is characterised by RMS values lower than 10 m/s. If the two valves are open, the largest RMS values move to region C, owing to the high interference between the fluxes from the intake valves, and the maximum is found at point 9 (16.4 m/s). In the “valve-valve interference” zone, a mean increase of about 30% in the RMS values is registered with respect to the configuration with only one valve open. On the other hand, points 12-13-14 and 1-2-3 exhibit RMS values always lower than 7.5 m/s.

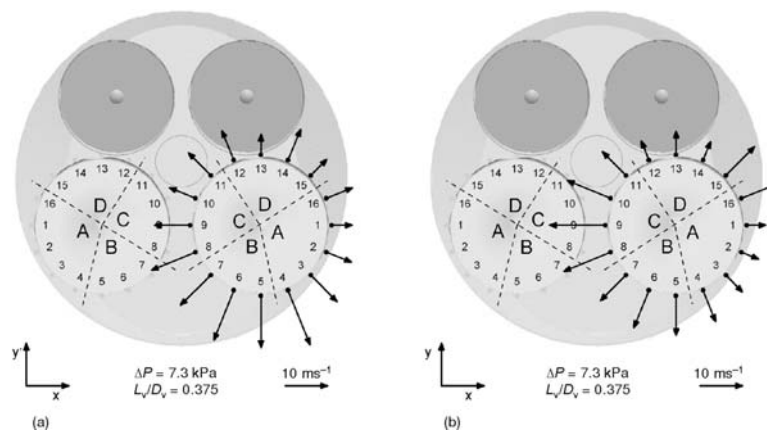


Figure 6. RMS velocity values around the intake valve for the configuration with only one valve open (a) and for the configuration with two valves open (b)

Finally, the comparison between the two engine configurations (one and both valves open) has been done considering the mean flow rates per sector. To this purpose, the height of the column bars in fig. 7 is proportional to the percentage volumetric flow rate per zone. The histogram shows clearly that the interference phenomena influence significantly the distribution of the flow around the valves. In fact, when the two intake valves are open, a noticeable decrease (larger than 8.3%) in sector C is present. At the same time, the plot put in evidence that the interference phenomena produce a redistribution of the flow around the valves, with the flow that tends towards the region where a larger degree of freedom is present. Consequently, a 4.4% increase in the mean flow rate is registered in the valve-wall interference zone (region A) and a slight upsurge is also evident in sector D (the forward-flow zone) and in sector B (the backward-flow zone), with a 2.1 and 1.8% raise, respectively.

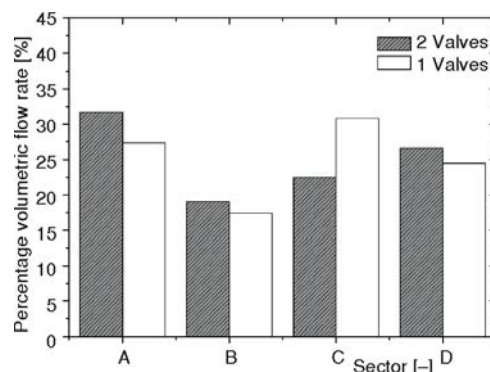


Figure 7. Influence of valve deactivation and interference phenomena on the percentage volumetric flow rate per sector

Conclusions

An experimental investigation has been carried out to characterise the fluid dynamic efficiency of a high performance ICE. Specifically, the work has been focused on a four-valve engine during the intake phase. To this purpose, measurements have been performed at a steady flow rig. Discharge coefficients have been used to characterise the global engine permeability while the LDA technique has been employed to give information on the flow distribution around the intake valve curtain area and on the interference phenomena between the two valves.

The global analysis has revealed the noticeable effect of the valve lift on the volumetric efficiency of the intake system. Specifically, different flow regimes have been observed and flow separation phenomena at the valve head and seat have been noticed at medium and high valve lifts.

Moreover, the analysis has highlighted that the valve-valve interference phenomena has a large effect on the engine head breathability. To this purpose, the dimensionless coefficients of the usual configuration with the two intake valves open have been compared with the results registered when an intake valve is deactivated. The absence of flow interactions between the two intake valves leads to a better filling of the cylinder when a single valve is open at low and medium valve lift. Conversely, at high valve lifts the configuration with both intake valves open presents better results due to the reduction in the flow irregularities at the bifurcation of the intake ducts.

Furthermore, LDA measurements have permitted the analysis of the flow field within the combustion chamber and the more detailed definition of the influence of the valve-valve interference phenomena. When only one valve is open, the mean flow appears quite uniform and the velocity direction is quite close to the radial direction. A distortion of the flow field and a significant decrease in the velocity magnitude have been found in region C when the two intake valves are open. Moreover, a redistribution of the flow along the entire valve periphery has been observed, with an increase in the regions A, B, and D. The analysis of the rms velocity distribution confirms the effect of the flow interference, with the highest values registered in the valve-valve interaction zone when the two intake valves are open.

Nomenclature

A	– area, [mm ²]
a	– sound speed, [ms ⁻¹]
B	– bore, [mm]
C_{abs}	– absolute flow coefficient, [-]
C_d	– discharge coefficient, [-]
D	– diameter, [mm]
D_v	– valve diameter, [mm]
L	– stroke, [mm]
L_v	– valve lift, [mm];
\dot{m}	– mass flow rate, [kgs ⁻¹]
N	– number, [-]
Δp	– ambient-cylinder pressure drop, [Pa]
p_0	– ambient pressure, [Pa]
p_C	– cylinder pressure, [Pa]
T_0	– ambient temperature, [°C]

Greek symbols

λ	– wavelength of the laser beam, [nm]
ρ	– air density, [kgm ⁻³]
ϕ_{Ad}	– dimensionless theoretical flow rate, [-]

ϕ_{Am}	– dimensionless actual flow rate, [-]
-------------	---------------------------------------

Subscripts

abs	– absolute
c	– cylinder
i	– intake
e	– exhaust
meas	– measured
r	– reference
v	– valve
0	– ambient

Acronyms

CFD	– computational fluid dynamics
DICP	– dual independent cam phasing
FFT	– fast Fourier transform
GDI	– gasoline direct injection
ICE	– internal combustion engine
LDA	– laser-Doppler anemometry
PIV	– particle image velocimetry

RMS – root mean square

WOT – wide open throttle

References

- [1] Heywood, J. B., *Internal Combustion Engine Fundamentals*, Mc Graw Hill, New York, USA, 1998
- [2] Jovanović, Z. S., *et al.*, The Effect of Combustion Chamber Geometry Lay-Out on Combustion and Emission, *Thermal Science*, 12 (2008), 1, pp. 7-24
- [3] Morrone, P., Algieri, A., Numerical Investigation on the Energetic Performances of Conventional and Pellet Aftertreatment Systems in Flow-Through and Reverse-Flow Designs, *Thermal Science*, 15 (2011), 4, pp. 1049-1064
- [4] Algieri, A., *et al.*, Energy Efficiency Analysis of Monolith and Pellet Emission Control Systems in Unidirectional and Reverse-Flow Designs, *SAE International Journal of Engines*, 2 (2010), 2, pp. 684-693
- [5] Barzegar, R., *et al.*, Combustion Fluid Dynamics Simulation of the Combustion Process, Emission Formation and the Flow Field in an In-Direct Injection Diesel Engine, *Thermal Science*, 17 (2013), 1, pp. 11-23, doi: 10.2298/TSCI111218108B (in this issue)
- [6] Zhijun, W., Zhen, H., In-Cylinder Swirl Formation Process in Four-Valve Diesel Engine, *Experiments in Fluids*, 31 (2001), 5, pp. 467-473
- [7] Jebamani, D. R., *et al.*, Studies on Variable Swirl Intake System for DI Diesel Engine Using Computational Fluid Dynamics, *Thermal Science*, 12 (2008), 1, pp. 25-32
- [8] Desantes, J. M., *et al.*, Air Mass Flow Estimation in Turbocharged Diesel Engines from In-Cylinder Pressure Measurement, *Experimental Thermal and Fluid Science*, 34 (2010), 1, pp. 37-47
- [9] Moore, W., *et al.*, Charge Motion Benefits of Valve Deactivation to Reduce Fuel Consumption and Emissions in a GDI, VVA Engine, SAE technical paper 2011-01-1221, 2011
- [10] Coltman, D., *et al.*, Project Sabre: A Close-Spaced Direct Injection 3-Cylinder Engine with Synergistic Technologies to Achieve Low CO₂ Output, SAE technical paper 2008-01-0138, 2008
- [11] Sellnau, M., *et al.*, 2-Step Variable Valve Actuation: System Optimization and Integration on an SI Engine, SAE technical paper 2006-01-0040, 2006
- [12] Patel, R., *et al.*, Un-Throttling a Direct Injection Gasoline Homogeneous Mixture Engine with Variable Valve Actuation, *International Journal of Engine Research*, 11 (2010), 6, pp. 391-411
- [13] Jemni, M. A., *et al.*, Influence of Intake Manifold Design on In-Cylinder Flow and Engine Performances in a Bus Diesel Engine Converted to LPG Gas Fuelled, Using CFD Analyses and Experimental Investigations, *Energy*, 36 (2011), 5, pp. 2701-2715
- [14] Jovanović, Z. S., *et al.*, The Effect of Bowl-In-Piston Geometry Layout on Fluid Flow Pattern, *Thermal Science*, 15 (2011), 3, pp. 817-832
- [15] Jasak, H., *et al.*, Rapid CFD Simulation of Internal Combustion Engines, SAE technical paper 1999-01-1185, 1999
- [16] Ramanathan, S., *et al.*, EGR and Swirl Distribution Analysis Using Coupled 1D-3D CFD Simulation for a Turbocharged Heavy Duty Diesel Engine, SAE technical paper 2011-01-2222, 2011
- [17] Kang, K. Y., Baek, J. H., LDV Measurement and Analysis of Tumble Formation and Decay in a Four-Valve Engine, *Experimental Thermal and Fluid Science*, 11 (1995), 2, pp. 181-189
- [18] Xu, H., Some Critical Technical Issues on the Steady Flow Testing of Cylinder Heads, SAE technical paper 2001-01-13, 2001
- [19] Pajković, V. R., Petrović, S. V., Spatial Flow Velocity Distribution around an Inlet Port/Valve Annulus, *Thermal Science*, 12 (2008), 1, pp. 73-83
- [20] Blair, G. P., *et al.*, Some Fundamental Aspects of the Discharge Coefficients of Cylinder Porting and Ducting Restrictions, SAE technical paper 980764, 1998
- [21] Blair, G. P., Drouin, F. M. M., Relationship between Discharge Coefficients and Accuracy of Engine Simulation, SAE technical paper 962527, 1996
- [22] Bohac, S. V., Landfaher, K., Effects of Pulsating Flow on Exhaust Port Flow Coefficients, SAE technical paper 1999-01-0214, 1999
- [23] Ismail, A. R., Bakar, R. A., Semin, Valve Flow Discharge Coefficient Investigation for Intake and Exhaust Port of Four Stroke Diesel Engines, *Journal of Engineering and Applied Sciences*, 2 (2007), 12, pp. 1807-1811
- [24] Son, J.-W., *et al.*, A Correlation Between Re-Defined Design Parameters and Flow Coefficients of SI Engine Intake Ports, SAE technical paper 2004-01-0998, 2004

- [25] Algieri, A., An Experimental Analysis of the Fluid Dynamic Efficiency of a Production Spark-Ignition Engine during the Intake and Exhaust Phase, *ISRN Mechanical Engineering*, 2011 (2011), ID427976
- [26] Ismail, A. R., *et al.*, Engine Power Calculation Using Air Flow through Engine from Flowbench Test Flow of Four Stroke Direct Injection Diesel Engines, *Journal of Engineering and Applied Sciences*, 2 (2007), 12, pp. 1812-1817
- [27] Chan, V. S. S., Turner, J. T., Velocity Measurement Inside a Motored Internal Combustion Engine Using Three-Component Laser-Doppler Anemometry, *Optics & Laser Technology*, 32 (2000), 7-8, pp. 557-566
- [28] Begg, S. M., *et al.*, Low Intake Valve Lift in a Port Fuel-Injected Engine, *Energy*, 34 (2009), 12, pp. 2042-2050
- [29] Krishna, B. M., Mallikarjuna, J. M., Characterization of Flow Through the Intake Valve of a Single Cylinder Engine Using Particle Image Velocimetry, *Journal of Applied Fluid Mechanics*, 3 (2010), 2, pp. 23-32
- [30] Bevan, K. E., Ghandhi, J. B., PIV Measurements of in-Cylinder Flow in a Four-Stroke Utility Engine and Correlation with Steady Flow Results, SAE technical paper 2004-32-0005, 2004
- [31] ***, Meriam, *Laminar Flow Elements – User Manual*, 2011
- [32] Auriemma, M., *et al.*, Fluid-Dynamic Analysis of the Intake System for a HDDI Diesel Engine by STAR-CD Code and LDA Technique, SAE technical paper n. 2003-01-0002, 2003
- [33] Doebelin, E. O., *Measurement System Application and Design*, Mc Graw Hill, New York, USA, 1990
- [34] Algieri, A., *et al.*, Experimental and Numerical Investigation on the Effects of the Seeding Properties on LDA Measurements, *Journal of Fluids Engineering*, 127 (2005), 3, pp. 514-522
- [35] Algieri, A., *et al.*, Influence of Valve-Lift and Throttle Angle on the Intake Process in High Performance Motorcycle Engine, *Journal of Engineering for Gas Turbine and Power*, 128 (2006), 4, pp. 934-941
- [36] Algieri, A., *et al.*, Numerical and Experimental Analysis of the Intake Flow in a High Performance Four-Stroke Motorcycle Engine, *Journal of Engineering for Gas Turbines and Power*, 129 (2007), 4, pp. 1095-1105
- [37] Weclas, M., *et al.*, Unsteady Intake Valve Gap Flow, SAE technical paper 952477, 1995